HHS Public Access

Author manuscript

Leukemia. Author manuscript; available in PMC 2022 October 01.

Published in final edited form as:

Leukemia. 2022 April ; 36(4): 1167–1170. doi:10.1038/s41375-022-01510-7.

Tcof1 haploinsufficiency promotes early T cell precursor-like leukemia in *Nras*$^{Q61R/+}$ mice

Zhi Wen[1,2], **Remington Finn**[1], **Xin Gao**[1], **Lin Li**[3], **Alexander Hebert**[4], **Erik A. Ranheim**[5], **Yun Zhou**[1], **Grant Yun**[1], **Jeroen P. Roose**[6], **Joshua J. Coon**[4,7,8], **Rita Shiang**[3], **Renren Wen**[9], **Menggang Yu**[10], **Demin Wang**[9,*], **Jing Zhang**[1,11,*]

[1]McArdle Laboratory for Cancer Research, University of Wisconsin-Madison, Madison, WI 53705, USA

[2]Center for Precision Medicine Research, Marshfield Clinic Research Institute, Marshfield Clinic Health System, Marshfield, WI 54449, USA

[3]Department of Human and Molecular Genetics, Virginia Commonwealth University, Richmond, VA 23298, USA

[4]National Center for Quantitative Biology of Complex Systems, University of Wisconsin-Madison, Madison, WI 53706, USA

[5]Department of Pathology & Laboratory Medicine, University of Wisconsin School of Medicine and Public Health, University of Wisconsin Carbone Cancer Center, Madison, WI 53792, USA

[6]Department of Anatomy, University of California-San Francisco, San Francisco, California 94143, USA

[7]Department of Biomolecular Chemistry, University of Wisconsin-Madison, Madison, WI 53706, USA

[8]Department of Chemistry, University of Wisconsin-Madison, Madison, WI 53706, USA

[9]Blood Research Institute, Versiti, Milwaukee, WI 53226, USA

[10]Department of Biostatistics and Medical Informatics, University of Wisconsin-Madison, Madison, WI 53706, USA

[*]**Corresponding authors: Demin Wang**, Address: Blood Research Institute, 8727 Watertown Plank Rd, Versiti, Milwaukee, WI 53226, Telephone: (414) 937-3874, dwang@versiti.org; **Jing Zhang**, Address: Wisconsin Institute for Medical Research II, McArdle Lab for Cancer Research, 1111 Highland Avenue, University of Wisconsin-Madison, Madison, WI 53705, Telephone: (608)263-1147, Fax: (608)262-2824, zhang@oncology.wisc.edu.

Author Contributions

Conception and design: Z. Wen, D. Wang, and J. Zhang

Acquisition of cell line and mouse data: Z. Wen, R. Finn and G. Yun

Analysis and interpretation of cell line and mouse data: Z. Wen, X. Gao, E. A. Ranheim, M. Yu, D. Wang, and J. Zhang

Acquisition and analysis of proteomic and phosphor-proteomic data: A. Hebert, J. J. Coon

Writing, review, and/or revision of the manuscript: Z. Wen, X. Gao, A. Hebert, E. A. Ranheim, J. J. Coon, R. Shiang, R. Wen, D. Wang, and J. Zhang

Technical or material support: L. Li, Y. Zhou

Study supervision: J. Zhang

Conflict of interest:

We declare that no conflict of interest exists.

Additional methods are described in Supplementary Materials and Methods.

[11]Wisconsin Blood Cancer Research Institute, University of Wisconsin-Madison, Madison, WI 53705, USA

Keywords

Tcof1; oncogenic Nras; ETP-like ALL; Rasgrp1; phospho-proteomics

Letter to the Editor

T-cell acute lymphoblastic leukemia (T-ALL) is a malignant neoplasm of transformed immature T-cells [1]. Recently, a refractory subset of T-ALL derived from the early T-cell precursors (ETPs) has been recognized and designated as ETP-ALL [2, 3]. ETP-ALL represents ~12% of T-ALL in children and 7.4% in adults, and confers a significantly worse outcome than other T-ALL subtypes (non-ETP T-ALL) [2]. ETP-ALL is characterized by distinct phenotypes, including simultaneous expression of myeloid or stem cell markers [2] and prevalent activating mutations in the Ras signaling pathway (e.g. *NRAS* and *KRAS*), which are rarely identified in non-ETP T-ALL but characteristic for myeloid leukemias [3].

Oncogenic *RAS* mutations predominantly occur at G12, G13, or Q61 codons, which compromise their GTPase activity and result in the accumulation of GTP-bound active Ras and hyperactivation of Ras downstream signaling [4]. In addition to the prevalent *NRAS* and *KRAS* mutations in ETP-ALL, we found concurrent oncogenic *RAS* mutations and haploinsufficiency of WT *KRAS* in some ETP-ALL patients. Notably, $Kras^{-/-}; Nras^{Q61R/+}$ mice developed early onset of T-cell malignancy that is characteristic of human ETP-ALL [5]. We showed that $Kras^{-/-}$ and $Nras^{Q61R}$ signaling cooperate to downregulate expression of *Rasgrp1*, a Ras guanine exchange factor [6]. *Rasgrp1* downregulation leads to hyperactivation of Nras/ERK signaling, T cell proliferation, and expansion of the ETP compartment. However, it remains unclear if *Rasgrp1* downregulation drives ETP-like ALL formation in $Nras^{Q61R/+}$ mice.

To address this question, we generated $Rasgrp1^{+/-}$; $Nras^{LSL\ Q61R/+}$; *Mx1-Cre* and $Rasgrp1^{-/-}; Nras^{LSL\ Q61R/+}$; *Mx1-Cre* mice and referred them as $Rasgrp1^{+/-}$; $Nras^{Q61R/+}$ and $Rasgrp1^{-/-}$; $Nras^{Q61R/+}$ mice respectively upon pI-pC treatment. Both groups of mice displayed *Rasgrp1* gene dosage-dependent survival, which was intermediate between $Nras^{Q61R/+}$ and $Kras^{-/-}$; $Nras^{Q61R/+}$ mice (Fig. S1a). At the moribund stage, only two of $Rasgrp1^{+/-}$; $Nras^{Q61R/+}$ mice displayed an enlarged thymus and died with ETP-like leukemia (Fig. S1b). Flow cytometry and pathological evaluation of hematopoietic tissues identified that additional two $Rasgrp1^{+/-}$; $Nras^{Q61R/+}$ mice and three $Rasgrp1^{-/-}$; $Nras^{Q61R/+}$ mice developed early stage of T-cell leukemia (Fig. S1c). Therefore, the incidences of T-cell disease in $Rasgrp1^{+/-}$; $Nras^{Q61R/+}$ mics (4/8) and $Rasgrp1^{-/-}$; $Nras^{Q61R/+}$ mice (3/5) were significantly higher than that in $Nras^{Q61R/+}$ mice (2/20) (Fig. S1d). In addition, we found that all the $Rasgrp1^{+/-}$; $Nras^{Q61R/+}$ and $Rasgrp1^{-/-}; Nras^{Q61R/+}$ mice developed myeloid disease (predominantly myeloproliferative neoplasm) (Fig. S2), similar as $Nras^{Q61R/+}$ mice[7], but with an accelerated rate. Some of them even showed transformation to acute myeloid leukemia. The rapid lethality in these mice may prevent the development of full-

blown T-cell malignancy. Collectively, our results indicate that *Rasgrp1* downregulation in *Nras*$^{Q61R/+}$ mice is capable but less potent than *Kras* downregulation to drive ETP leukemic transformation. We postulated that additional mediator(s) may be critical to promote the early onset of T-cell malignancy in *Kras*$^{-/-}$; *Nras*$^{Q61R/+}$ mice.

To identify novel molecular event(s) that facilitate(s) the initiation of ETP-like ALL in *Kras*$^{-/-}$; *Nras*$^{Q61R/+}$ mice, we collected thymocytes from control, *Nras*$^{Q61R/+}$, and *Kras*$^{-/-}$; *Nras*$^{Q61R/+}$ mice as previously described [5] and conducted a quantitative phospho-proteomics and proteomics study (Fig. 1a). These quantitative analyses revealed that the level of phosphorated Tcof1 at T104 was significantly downregulated in *Kras*$^{-/-}$; *Nras*$^{Q61R/+}$ thymocytes as compared to control and *Nras*$^{Q61R/+}$ thymocytes, while the total level of Tcof1 protein was comparable among all three groups (Fig. 1b and 1c). *TCOF1* plays a critical role in craniofacial development and its mutations cause Treacher Collins syndrome in humans [7, 8]. *TCOF1* is located in human chromosome 5q region that is deleted in a subset of myelodysplastic syndrome patients. A recurrent *TCOF1* somatic mutation was previously identified in *de novo* acute myeloid leukemia with monocytic differentiation [9]. However, the function of TCOF1 in hematopoiesis or leukemogenesis has not been studied before. Interestingly, *Tocf1* displays a similar expression pattern to *Rasgrp1* and *Ets1* [5] during T cell development, low at the ETP stage and higher following T cell maturation (Fig. S3). Moreover, alignment of TCOF1 protein sequences from human, rabbit, monkey, and mouse demonstrated that T104 and its adjacent amino acids are highly conserved in these species (Fig. 1d), suggesting that phosphorylation at T104 is likely to have an important role in regulating Tcof1 function.

To determine whether phosphorylation at human TCOF1 T102 (corresponding to mouse T104) plays a functional role, we overexpressed wild-type (WT) TCOF1, phosphorylation-deficient TCOF1 T102A, and phosphorylation-mimicking TCOF1 T102D in human Jurkat T cells. Interestingly, overexpression of TCOF1 T102D moderately but significantly decreased the percentage of Jurkat cells in S-phase, while no effects were observed with WT and T102A TCOF1 overexpression (Fig. S4a). It is possible that both WT and T102A TCOF1 do not have a dominant function in cell cycle progression in the presence of endogenous TCOF1. By contrast, sh*TCOF1* decreased endogenous TCOF1 protein level, leading to a moderate increase of Jurkat cells in S-phase (Fig. S4b). Our results demonstrate that human TCOF1 is regulated through T102 and that TCOF1 levels impact cell cycle progression in the Jurkat T cell line model.

Consistent with our Jurkat data, our prior RNA-Seq analysis showed that *Tcof1* mRNA level in *Kras*$^{-/-}$; *Nras*$^{Q61R/+}$ ETP-like ALL cells was lower than that in control thymocytes (data not shown). We validated this observation using RT-qPCR (Fig. 1e). More importantly, *TCOF1* mutations, predominantly haploinsufficiency, were more prevalent in human ETP-ALL patients as compared to T-ALL patients (Fig. 1f). Corroborating our mouse result, *TCOF1* mRNA levels were lower in human ETP-ALL cells *vs* T-ALL (Fig. 1g), suggesting that *TCOF1* downregulation might play an important role in ETP-ALL development.

To validate the role of *Tcof1* downregulation in ETP-ALL, we generated *Tcof1* conditional knockout allele and subsequently *Tcof1*$^{fl/+}$*; Mx1-Cre* and *Tcof1*$^{fl/+}$*; Nras*$^{LSL\ Q61R/+}$*; Mx1-*

Cre mice (Fig. 2a). We referred them as *Tcof1*$^{+/-}$ and *Tcof1*$^{+/-}$; *Nras*$^{Q61R/+}$ mice upon pI-pC treatment. pI-pC injections efficiently induced deletion of the floxed *Tcof1* allele and activation of oncogenic *Nras* in *Tcof1*$^{+/-}$; *Nras*$^{Q61R/+}$ thymocytes (Fig. 2b). Consistent with our Jurkat data, *Tcof1*$^{+/-}$; *Nras*$^{Q61R/+}$ Thy1.2^{+} cKit^{+} thymocytes were more proliferative than control cells on Day 37 (Fig. 2c). More importantly, *Tcof1*$^{+/-}$; *Nras*$^{Q61R/+}$ mice showed a significantly shortened survival compared to *Nras*$^{Q61R/+}$ mice (Fig. 2d) with a marked increase of T cell malignancy incidence as indicated by their enlarged thymi (Fig. 2e). Similar to the ETP-like leukemia cells in *Kras*$^{-/-}$; *Nras*$^{Q61R/+}$ mice, the malignant T cells in *Tcof1*$^{+/-}$; *Nras*$^{Q61R/+}$ mice behaved aggressively with frequent infiltration of the bone marrow and spleen (Fig. 2f). Interestingly, at the moribund stage, Tcof1 protein levels were greatly decreased in *Tcof1*$^{+/-}$; *Nras*$^{Q61R/+}$ thymocytes (Fig. 2g). Detailed immunophenotypic analyses showed that the number of Thy1.2^{+} Mac1^{+} T lymphoblasts significantly increased in *Tcof1*$^{+/-}$; *Nras*$^{Q61R/+}$ mice compared to those in age-matched control, *Tcof1*$^{+/-}$, and *Nras*$^{Q61R/+}$ mice (Fig. 2h). We also quantified ETP cells in all groups of animals as CD4, CD8-double negative (DN)1, cKit^{+} DN1, or cKit^{+} DN1+DN2 as in our prior study [5]. Regardless of ETP definitions, we observed a marked expansion of the ETP compartment in *Nras*$^{Q61R/+}$ mice compared to control and *Tcof1*$^{+/-}$ mice, and a further expansion in *Tcof1*$^{+/-}$; *Nras*$^{Q61R/+}$ mice over *Nras*$^{Q61R/+}$ mice (Figure 2i). Taken together, our data demonstrated that *Tcof1*$^{+/-}$ promotes ETP expansion and ETP-like leukemia in *Nras*$^{Q61R/+}$ mice.

In summary, our quantitative phospho-proteomics identified reduced Tcof1 phosphorylation at the conserved T104 codon in *Kras*$^{-/-}$; *Nras*$^{Q61R/+}$ thymocytes at the early stage, while Tcof1 downregulation was observed in both mouse and human ETP-ALL cells. More importantly, *Tcof1* haploinsufficiency promoted ETP proliferation and expansion, leading to an increased incidence of ETP-like ALL in *Nras*$^{Q61R/+}$ mice. Our study identified *Tcof1* as a novel regulator in oncogenic *Nras*-driven ETP-like leukemia.

Methods

Mice.

All mouse lines were maintained in a pure C57BL/6J genetic background (>N10). The *Tcof1* conditional knockout allele was constructed as illustrated in Fig. 2a. The conditional allele was confirmed by PCR genotyping using the following primer set: TLoxPF (5’-cac tag tga cat ctc atg cc-3’) and TLoxPR (5’-aag gct aac tag ctc tgc ca-3’). The wild-type allele produces a 266-bp product whereas the floxed allele product is 300-bp. A second primer set consisting of TLoxPF and TdelR (5’-gca ggc aga tct ctg agt tc-3’) was used to detect a 375-bp product, indicating the Cre-mediated *Tcof1* deletion.

Supplementary Material

Refer to Web version on PubMed Central for supplementary material.

Acknowledgements

We would like to thank the University of Wisconsin Carbone Comprehensive Cancer Center (UWCCC) for use of its Shared Services (Flow Cytometry Laboratory, Transgenic Animal Facility, and Experimental Pathology

Laboratory) to complete this research. This work was supported by the startup funding from the Marshfield Clinic Research Foundation to Z.W., NIH grant P41 GM108538 to A. H. and J. J. C., NIH grant R01DE13172 to L.L. and R.S., NIH grants R01CA187318 and R01HL120724 to J.P.R., NIH grants R01AI079087 and R01HL130724 to D.W., and NIH grant R01CA152108 and DoD Impact Award W81XWH-20-1-0616 to J.Z. This work was also supported in part by NIH/NCI P30 CA014520--UW Comprehensive Cancer Center Support.

References

1. Girardi T, Vicente C, Cools J, De Keersmaecker K. The genetics and molecular biology of T-ALL. Blood 2017 Mar 2; 129(9): 1113–1123. [PubMed: 28115373]
2. Coustan-Smith E, Mullighan CG, Onciu M, Behm FG, Raimondi SC, Pei D, et al. Early T-cell precursor leukaemia: a subtype of very high-risk acute lymphoblastic leukaemia. Lancet Oncol 2009 Feb; 10(2): 147–156. [PubMed: 19147408]
3. Zhang J, Ding L, Holmfeldt L, Wu G, Heatley SL, Payne-Turner D, et al. The genetic basis of early T-cell precursor acute lymphoblastic leukaemia. Nature 2012 Jan 11; 481(7380): 157–163. [PubMed: 22237106]
4. Simanshu DK, Nissley DV, McCormick F. RAS Proteins and Their Regulators in Human Disease. Cell 2017 Jun 29; 170(1): 17–33. [PubMed: 28666118]
5. Wen Z, Yun G, Hebert A, Kong G, Ranheim EA, Finn R, et al. Nras Q61R/+ and Kras−/− cooperate to downregulate Rasgrp1 and promote lympho-myeloid leukemia in early T-cell precursors. Blood 2021 Jun 10; 137(23): 3259–3271. [PubMed: 33512434]
6. Ksionda O, Limnander A, Roose JP. RasGRP Ras guanine nucleotide exchange factors in cancer. Front Biol (Beijing) 2013 Oct 1; 8(5): 508–532. [PubMed: 24744772]
7. Kong G, Chang YI, You X, Ranheim EA, Zhou Y, Burd CE, et al. The ability of endogenous Nras oncogenes to initiate leukemia is codon-dependent. Leukemia 2016 Sep; 30(9): 1935–1938. [PubMed: 27109513]
8. Jones NC, Lynn ML, Gaudenz K, Sakai D, Aoto K, Rey JP, et al. Prevention of the neurocristopathy Treacher Collins syndrome through inhibition of p53 function. Nat Med 2008 Feb; 14(2): 125–133. [PubMed: 18246078]
9. Marszalek B, Wojcicki P, Kobus K, Trzeciak WH. Clinical features, treatment and genetic background of Treacher Collins syndrome. J Appl Genet 2002; 43(2): 223–233. [PubMed: 12080178]
10. Yan XJ, Xu J, Gu ZH, Pan CM, Lu G, Shen Y, et al. Exome sequencing identifies somatic mutations of DNA methyltransferase gene DNMT3A in acute monocytic leukemia. Nat Genet 2011 Mar 13; 43(4): 309–315. [PubMed: 21399634]

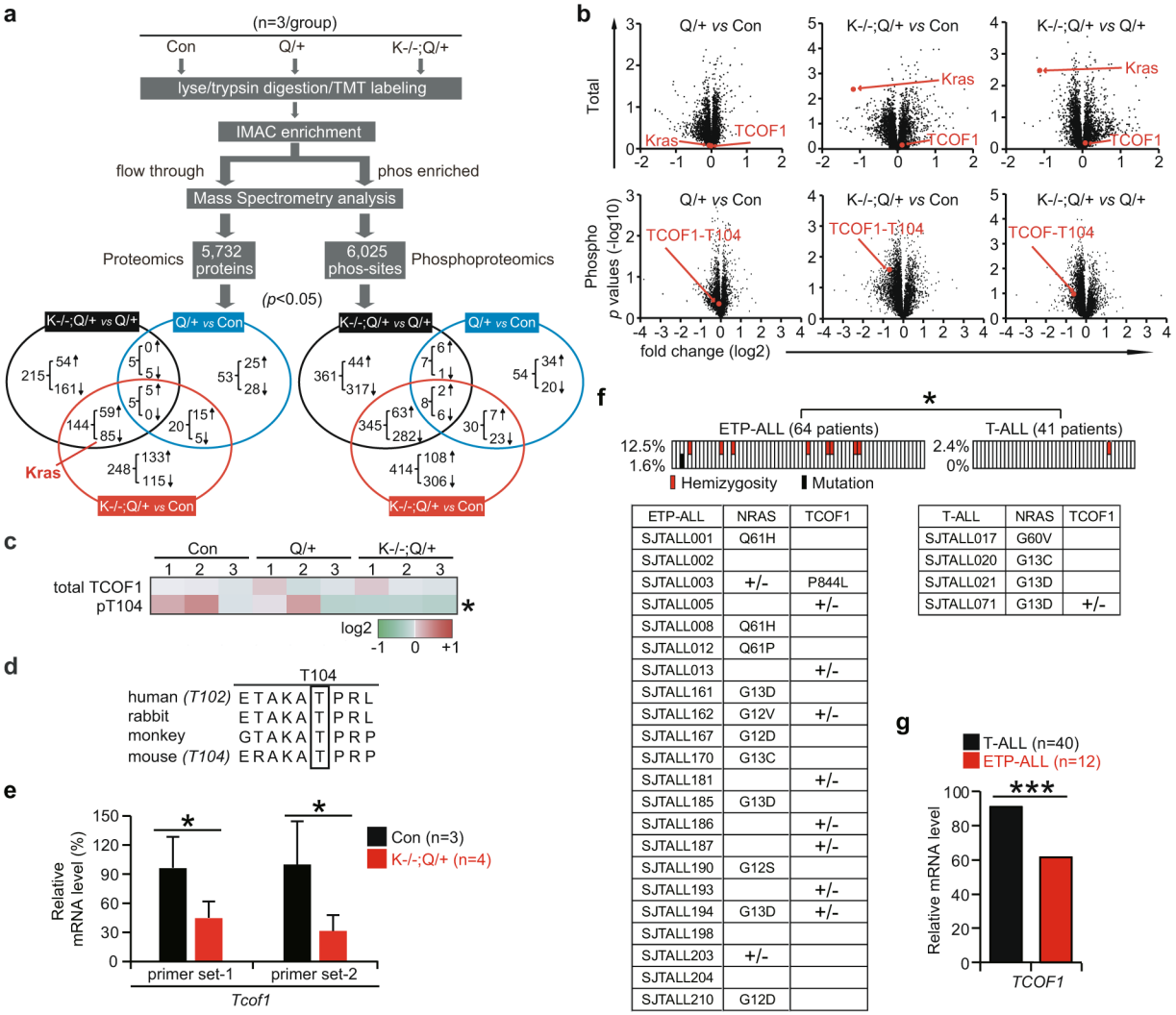

ETP-ALL	NRAS	TCOF1
SJTALL001	Q61H	
SJTALL002		
SJTALL003	+/-	P844L
SJTALL005		+/-
SJTALL008	Q61H	
SJTALL012	Q61P	
SJTALL013		+/-
SJTALL161	G13D	
SJTALL162	G12V	+/-
SJTALL167	G12D	
SJTALL170	G13C	
SJTALL181		+/-
SJTALL185	G13D	
SJTALL186		+/-
SJTALL187		+/-
SJTALL190	G12S	
SJTALL193		+/-
SJTALL194	G13D	+/-
SJTALL198		
SJTALL203	+/-	
SJTALL204		
SJTALL210	G12D	

T-ALL	NRAS	TCOF1
SJTALL017	G60V	
SJTALL020	G13C	
SJTALL021	G13D	
SJTALL071	G13D	+/-

Figure 1. Quantitative phospho-proteomics and RNA-Seq analyses identify *Tocf1* as a potential regulator of *Kras*$^{-/-}$;*Nras*$^{Q61R/+}$-induced ETP-like leukemia.

(a-c) Six-seven weeks old *Mx1-Cre* (Con), *Nras*$^{Q61R/+}$ (Q/+), and *Kras*$^{-/-}$; *Nras*$^{Q61R/+}$ (K−/−; Q/+) mice were treated with pI-pC as described in Materials and Methods. Thymocytes were collected ~4 weeks after the last pI-pC injection for quantitative phospho-proteomics and proteomics analyses. (a) Flow chart of quantitative phospho-proteomics and proteomics studies of thymocytes (n=3 per group). *p* values were calculated using student's t-Test with two-tails. Peptides with $p<0.05$ were selected for bioinformatics analysis. (b) Volcano plot analysis of total peptides (upper) and phosphorylated peptides (lower) in the quantitative proteomics and phospho-proteomics studies, respectively. The x-axis represents fold-change of total or phosphorylated peptides (log2) in Q/+ *vs* control, K−/−; Q/+ *vs* control, and K−/−; Q/+ *vs* Q/+, and the y-axis represents *p* values (−log10). (c) Heat map of total Tcof1 and phosphorylated Tcof1 T104 levels in Con, Q/+, and K−/−; Q/+ thymocytes. (d) Alignment of Tcof1 peptide sequence containing T104 among different species. The rectangle defines the highly conserved phosphorylation site. (e) qRT-PCR quantification of *Tcof1* mRNA in thymocytes from moribund K−/−; Q/+ mice and age-matched controls

using two different primer sets. *p* values were calculated with student's t-Test with two-tails. (f) *TCOF1* mutations in human ETP-ALL and T-ALL samples. Chi-square analysis was performed. (g) Quantification of *TCOF1* mRNA levels in human ETP-ALL and T-ALL samples. *p* value was cited from the original study [5]. * $p<0.05$; *** $p<0.001$.

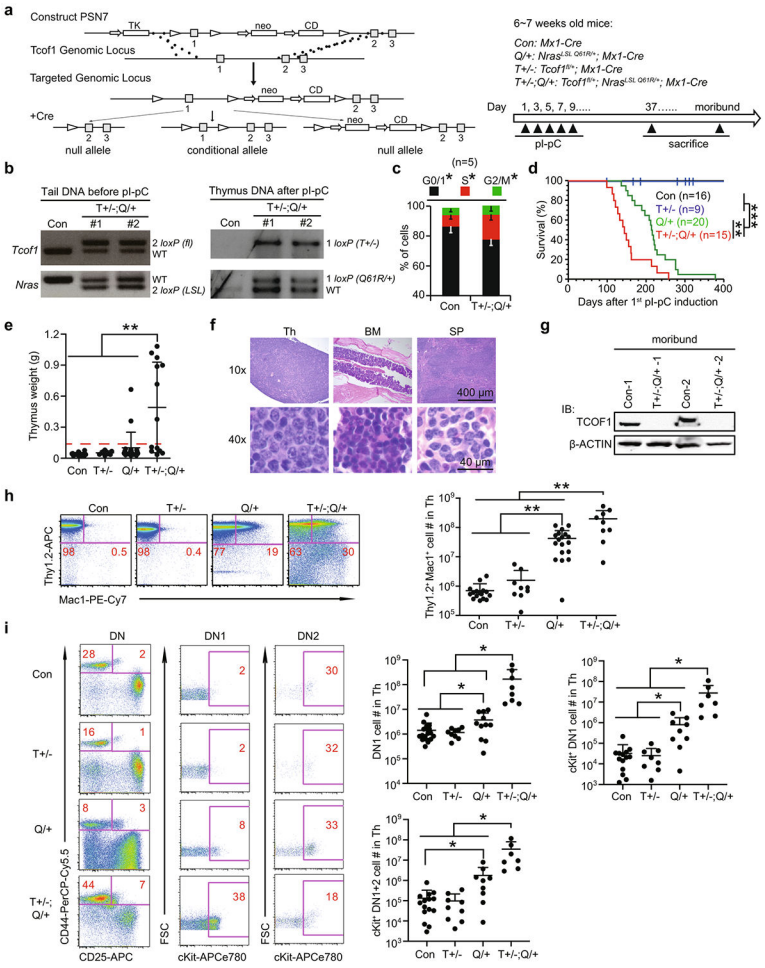

Figure 2. *Tcof1* haploinsufficiency promotes expansion of early T-cell precursors and an early on-set of ETP-like ALL in *Nras*$^{Q61R/+}$ mice.

Six-seven weeks old *Mx1-Cre* (Con), *Nras*$^{Q61R/+}$ (Q/+), *Tcof1*$^{+/-}$ (T+/−), and *Tcof1*$^{+/-}$*; Nras*$^{Q61R/+}$ (T+/−; Q/+) mice were treated with pI-pC as described in Materials and Methods. Thymocytes were collected ~4 weeks after the last pI-pC injection for Day 37 and moribund stage analyses. (a) Schematic illustration of constructing the conditional *Tcof1* knockout allele (*left*) and the experimental scheme (*right*). (b) Genotyping of *Tcof1* and *Nras* alleles in T+/−; Q/+ mice before and after pI-pC induction. (c) Cell cycle analysis of Thy1.2^{+} cKit^{+} thymocytes on Day 37. (d) Kaplan-Meier survival curves were plotted against days after the 1st pI-pC injection. *p* values were calculated using the Log-rank test. (**e**) Quantification of thymus weight. T cell malignancy is defined as thymus weight above 150 mg (red dashed line). (f) Representative H&E stained images of hematopoietic tissues from moribund T+/−; Q/+ mice. (g) Western blot analysis of Tcof1 protein levels in thymocytes from the moribund T+/−; Q/+ mice and age-matched control mice. (h) Quantification of the number of Thy1.2^{+} Macl^{+} thymocytes. (i) Quantification of the number of early T-cell precursors. DN, CD4^{-} CD8^{-} T cells; DN1, CD44^{+} CD25^{-} DN cells; DN2, CD44^{+} CD25^{+} DN cells. Data are plotted as mean + SD. *p* values were calculated with student's t-Test with two-tails. * $p<0.05$; ** $p<0.01$; *** $p<0.001$.